FSMILE 2020

November 24-25, 2020

Effect of steaming on lipid profile of tilapia muscles

R. Sun,T.T. Wu, N.P. Tao, X.C. Wang, J. Zhong*

National R&D Branch Center for Freshwater Aquatic Products Processing Technology (Shanghai), Integrated Scientific Research Base on Comprehensive Utilization Technology for By-Products of Aquatic Product Processing, Ministry of Agriculture and Rural Affairs of the People's Republic of China, Shanghai Engineering Research Center of Aquatic-Product Processing and Preservation, College of Food Science and Technology, Shanghai Ocean University, Shanghai 201306, China

Contact Information:

First author, 2983465575@qq.com, *Corresponding author, jzhong@shou.edu.cn

INTRODUCTION

Tilapia

- **Fast growth speed** & adapt ability to a wide range of environmental conditions.
- **Ability to grow and reproduce in captivity** & easy feed on low trophic level.
- Easy processing to fish fillets & especially suitable foe the elderly and children.
- **Low fat high protein rich in unstaturated fatty acids.**

AIM

- Through the thermal processing method of steaming, the lipid in tilapia meat is extracted, and the optimal thermal processing time of tilapia steaming is determined to **retain more nutrients** and **increase the edible value**.
- Analyze **the distribution of complex lipids and free fatty acids** in tilapia meat and determine the effects of complex lipids and free fatty acids on the **nutrition, flavor and appearance** of tilapia meat.
- **Use lipidomics to explain the changes of tilapia meat lipids and free fatty acids and lay the theoretical foundation for lipidomics**.
- Better application in the processing industry of tilapia, making the thermal processing of tilapia more industrialized.

METHOD

- **Thawing andThermal processing**

Thaw the tilapia fillets at room temperature, dry the surface water .Use an induction cooker to heat the water in the pot until it boils, then add the fish, use the steaming mode to heat, take out the fish at different time periods, cool, weigh, and beat into surimi.

- **Lipid extraction**

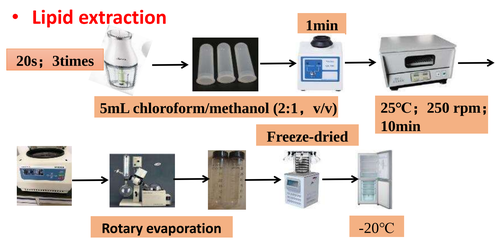

- **LC-MS Detections**

5 mL chloroform/methanol (2:1, v/v) was added into the tubes to dissolve the lipid films on the tube wall. Then the samples were detected by the UPLC-Q-Extractive Orbitrap mass spectrometer with a heated electrospray ionization probe.

- **Statistics**

Peak areas of compound lipids were extracted using software LipidSearch 4.0 . Peak areas of free DHA, EPA, and ARA were extracted using software Xcalibur 3.2.63.The data sets were then imported in MetaboAnalyst 4.0 in which the data were analyzed.

RESULTS

1.In the negative ionization mode, the detected lipids include Cer , CL , FA , LPC , LPE , LPI , OAHFA , PC , PE , PEt , SM and 11 lipid subclasses. In the positive ionization mode, the detection There are 8 lipid subclasses: AcCa , Cer , LPC , LPE , PC , PE , SM and TG.

2. In the negative ionization mode, Cer, CL , LPC , LPI , PC , PE , SM , a total of 7 lipid subclasses appear regularly, in the positive ionization mode, only PC and TG, a total of 2 lipid subclasses appear regularly.

3.Certain lipid subclasses suddenly begin to appear in a certain period of time with the extension of heating time, for example: FA, LPE, OAHFA, PEt in negative ionization mode, LPC, LPE or in a positive ionization mode Suddenly disappear for a period of time, such as AcCa, Cer, SM in the positive ionization mode, which may be due to the transformation phenomenon during the heating process. In addition, in terms of the growth geographical environment and growth time of the tilapia, it is The type of lipid in the fish may also have an effect.

4. After merging the lipid subclasses of complex lipids, it is found that the peak area of most lipids increases first and then decreases with the extension of heating time, indicating that some lipids have increased with the extension of heating time. The substance may be transformed into other lipids, or lipids in the form of lipoproteins and glycolipids are lost to the fish soup through water during the heating process, resulting in a decrease in lipid content.

Table1. Under the positive and negative ionization mode, the names of lipid subclasses appearing in different time periods.

LipidMolec	Negative Ionization 0min	10min	20min	60min
Cer	Cer	Cer	Cer	Cer
CL	CL	CL	CL	CL
FA		FA	FA	FA
LPC	LPC	LPC	LPC	LPC
LPE			LPE	LPE
LPI	LPI	LPI	LPI	LPI
OAHFA		OAHFA	OAHFA	OAHFA
PC	PC	PC	PC	PC
PE	PE	PE	PE	PE
PEt		PEt	PEt	PEt
SM	SM	SM	SM	SM

LipidMolec	Positive Ionization 0min	10min	20min	60min
AcCa	AcCa			
Cer	Cer	Cer	Cer	
LPC		LPC	LPC	LPC
LPE			LPE	LPE
PC	PC	PC	PC	PC
PE	PE		PE	PE
SM	SM	SM	SM	
TG	TG	TG	TG	TG

Table 2. Summary of the peak areas of lipid subclasses in different time periods. [c], [s2], [s3], [s5] represent the heating time of 0min, 10min, 20min, and 60min respectively.

Class	MainArea[c]	MainArea[s2]	MainArea[s3]	MainArea[s5]
Cer	2.35E+08	7.68E+07	3.27E+08	6.21E+06
CL	1.36E+07	1.47E+07	7.11E+06	1.52E+07
FA		7.57E+09	8.13E+09	1.21E+10
LPC	9.04E+07	6.24E+08	1.14E+09	5.51E+08
LPE			1.18E+08	8.42E+07
LPI	4.88E+06	5.36E+06	6.19E+06	1.08E+07
OAHFA		1.66E+07	7.77E+07	4.79E+07
PC	1.18E+09	1.63E+08	1.14E+09	1.52E+08
PE	1.30E+09	1.70E+08	3.42E+08	5.97E+08
PEt		7.65E+06	1.24E+07	2.32E+07
SM	1.98E+08	8.70E+08	9.96E+08	2.72E+08

Class	MainArea[c]	MainArea[s2]	MainArea[s3]	MainArea[s5]
AcCa	1.12E+06			
Cer	3.23E+07	3.55E+07	1.40E+07	
LPC		2.24E+09	1.22E+10	1.26E+10
LPE			9.96E+07	1.18E+08
PC	1.44E+10	2.35E+10	1.04E+10	8.20E+08
PE	1.86E+08		2.27E+10	2.87E+08
SM	9.92E+08	3.87E+09	4.54E+10	
TG	6.21E+10	2.23E+11	1.36E+11	6.65E+09

CONCLUSIONS

Through thermal processing of tilapia, 1).the distribution of lipid species in different time periods is obtained. In the positive and negative ionization mode, **Cer, CL, FA, LPC, LPE, LPI, OAHFA, PC, PE, PEt, SM** The regular appearance of TG and TG in the thermal processing of fish meat indicates that it is in a relatively stable state during the thermal processing and is not easily oxidized.2). When the heating time is 20 minutes, the most lipid types appear in the positive and negative ionization mode. As the heating time increases, the lipid types in the whole fish meat show a trend of first increasing and then decreasing, indicating that tilapia meat is in this experiment The best processing time is 20min.3). Using lipidomics theory to explore the changes in tilapia lipids in order to discover the changes in lipids in tilapia after steaming, and analyze the changes in complex lipids in the body, which is better and more valuable for people Edible tilapia and tilapia meat play a very important role in the nutrition, flavor, texture, and appearance of the processing process and the development of the entire aquatic product processing industry.

ACKNOWLEDGEMENTS

This research has been supported by research grants from the National Key R&D Program (2019YFD0902003), and Shanghai Municipal Education Commission—Gaoyuan Discipline of Food Science & Technology Grant Support (Shanghai Ocean University).

REFERENCES

[1]Shi C , Guo H , Wu T , et al. Effect of three types of thermal processing methods on the lipidomics profile of tilapia fillets by UPLC-Q-Extractive Orbitrap mass spectrometry[J]. Food Chemistry, 2019, 298(NOV.15):125029.

[2]Wu T , Zhao J , Ding M , et al. Preparation of selected spice microparticles and their potential application as nitrite scavenging agents in cured Tilapia muscle[J]. International Journal of Food ence And Technology, 2020, 55(9):3153-3161.

[3]A T W , B H G , C Z L , et al. Reliability of LipidSearch software identification and its application to assess the effect of dry salting on the long-chain free fatty acid profile of tilapia muscles - ScienceDirect[J]. Food Research International, 138.

FSMILE 2020

November 24-25, 2020

Ionotropic Gelation Electrospraying Technique for the Preparation of Multicore Millimeter-Sized Spherical Capsules to Specifically and Sustainedly Release Fish Oil

L.N. Tao, P.P. Wang, T. Zhang, M.Z. Ding, L.J. Liu, N.P. Tao, X.C. Wang, J. Zhong*

National R&D Branch Center for Freshwater Aquatic Products Processing Technology (Shanghai), Integrated Scientific Research Base on Comprehensive Utilization Technology for By-Products of Aquatic Product Processing, Ministry of Agriculture and Rural Affairs of the People's Republic of China, Shanghai Engineering Research Center of Aquatic-Product Processing and Preservation, College of Food Science and Technology, Shanghai Ocean University, Shanghai 201306, China

Contact Information:
First author, taolina1995@163.com,
*Corresponding author, jzhong@shou.edu.cn

INTRODUCTION

Multiscale encapsulation techniques have become one of the hot spots in food and pharmaceutical industry due to their huge advantages for active substances. Centimeter-sized capsules are difficult to be swallowed for some people. Micro/nano capsules have low stability for active substances due to their sizes. In addition, specific and sustained delivery behaviors are also important requirements for active substance delivery in human organs . Therefore, it is meaningful to develop **millimeter-sized particles with specific and sustained release behaviors** to meet the release requirements of some food and drug active substances.

AIM

The objective of this study is to prepare multicore millimeter-sized spherical capsules for specific and sustained release of fish oil by ionotropic gelation electrospraying technique.

METHOD

Alginate gel-stabilized fish oil droplet solution was prepared and used to prepare millimeter-sized spherical capsules using electrospraying technique.

- **The capsule shapes** were photographed by a digital camera, an upright optical microscope, a confocal laser scanning microscope, and a scanning electron microscope
- **The fish oil loading ratios** of the millimeter-sized spherical capsules were measured.
- **The fish oil sustained release behaviors** of the millimeter-sized capsules in the in vitro digestion models were determined.

RESULTS

As shown in the DC images in Figure 1 , capsule sizes decreased with the increase of applied voltages. The diameters of spherical capsules could be of 0.35-2.05 mm.The OM images in Figure 1 showed there were many light spots in the capsules, which were more obviously at higher voltages. Scanning electron microscopy images (Figure 2) showed that there were many hemisphere-like humps on the surface of capsules. 3D reconstructed CLSM image (Figure 3) demonstrated that fish oils were uniformly and non-continuously distributed on the surface of the capsules. Therefore, the multicore capsules could be classified into even and uneven multicore capsules.

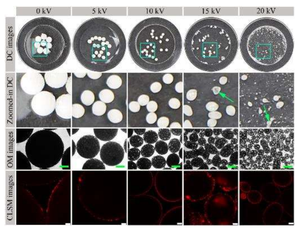

fig.1 DC, OM, and CLSM images of capsules prepared at different voltages

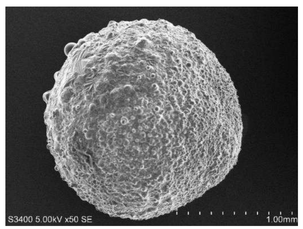

fig.2 Scanning electron microscopy image of capsule

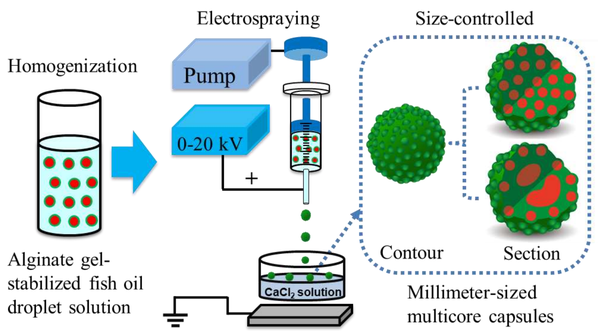

fig.6 Schematics of ionotropic gelation electrospraying technique for the preparation of fish oil-loaded millimeter-sized even and uneven multicore spherical capsules.

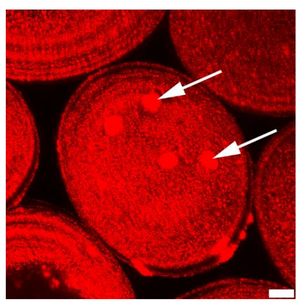

fig.3 3D reconstructed CLSM image of capsule

As shown in Figure 4, the loading ratio of the capsules prepared at 0 kV was 9.7% ± 1.7%. The applied voltages (5 – 20 kV) slightly decreased the loading ratios to 7.1% – 6.3% and they had no obvious differences in the loading ratios.

The fish oils were sustainedly released from the capsules without obvious burst release and the released amounts increased with the increase of applied voltages. It is reasonable because the multicores were uneven at higher applied voltages (Figure 5).

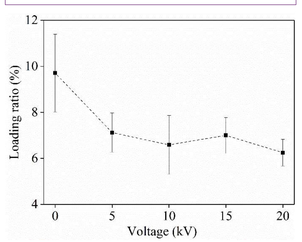

fig.4 The fish oil loading ratios

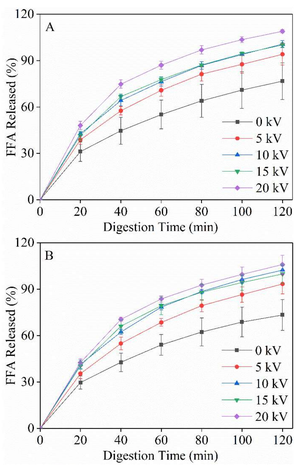

fig.5 Calculated FFA release from the fish oil-loaded millimeter-sized capsules during in vitro digestion in the small intestinal phases of the gastro-intestinal tract model (A) and the small intestinal model (B).

CONCLUSIONS

The diameters of spherical capsules could be controlled from 0.35 mm to 2.05 mm by adjusting the applied voltages. The millimeter-sized multicore spherical capsules could be classified into two types: (1) even multicore capsules; (2) uneven multicore capsules. The millimeter-sized capsules had reasonable fish oil loading ratios and fish oils could be specifically and sustainedly released in the small intestinal phase of in vitro gastro-intestinal and small intestinal tract models. Moreover, the sustained release behaviors could be controlled by the applied voltages. Conversion of liquid fish oil to solid capsules was achieved for easy processing and storage.

ACKNOWLEDGEMENTS

This research has been supported by research grants from the National Key R&D Program (2019YFD0902003), and Shanghai Municipal Education Commission—Gaoyuan Discipline of Food Science & Technology Grant Support (Shanghai Ocean University).

REFERENCES

[1] Chen, S., Li, R., Li, X., & Xie, J. (2018). Electrospinning: An enabling nanotechnology platform for drug delivery and regenerative medicine. Advanced Drug Delivery Reviews, 132, 188-213.

[2] Sun, G., Wei, D., Liu, X., Chen, Y., Li, M., He, D., & Zhong, J. (2013). Novel biodegradable electrospun nanofibrous P(DLLA-CL) balloons for the treatment of vertebral compression fractures. Nanomedicine-Nanotechnology Biology and Medicine, 9, 829-838.

[3] Wang, P., Li, M., Wei, D., Ding, M., Tao, L., Liu, X., Zhang, F., Tao, N., Wang, X., Gao, M., & Zhong, J. (2020). Electrosprayed soft capsules of millimeter-size for specifically delivering fish oil/nutrients to stomach and intestines. ACS Applied Materials & Interfaces, DOI: 10.1021/acsami.9b23623.

[4] Zhang, N., Qiao, R., Su, J., Yan, J., Xie, Z., Qiao, Y., Wang, X., & Zhong, J. (2017). Recent advances of electrospun nanofibrous membranes in the development of chemosensors for heavy metal detection. Small, 13, 1604293.

[5] Zhang, N., Wang, X., Ma, C., Qiao, Y., Zhang, H., Shi, C., Zhou, X., Zhang, Y., Qiao, R., Wang, X., & Zhong, J. (2019). Electrospun nanofibrous cellulose acetate/curcumin membranes for fast detection of Pb ions. Journal of Nanoscience and Nanotechology, 19, 670-674.

[6] Zhang, T., Ding, M., Zhang, H., Tao, N., Wang, X., & Zhong, J. (2020). Fish oil-loaded emulsions stabilized by synergetic or competitive adsorption of gelatin and surfactants on oil/water interfaces. Food Chemistry, 308, 125597.

FSMILE 2020

November 24-25, 2020

Preparation and characterization of gelatin/Vitamin C core-shell nanofibers based on electrospinning technology

L.J. Liu, L.N. Tao, T. Zhang, M.Z. Ding, P.P. Wang, N.P. Tao, X.C. Wang, J. Zhong*

National R&D Branch Center for Freshwater Aquatic Products Processing Technology (Shanghai), Integrated Scientific Research Base on Comprehensive Utilization Technology for By-Products of Aquatic Product Processing, Ministry of Agriculture and Rural Affairs of the People's Republic of China, Shanghai Engineering Research Center of Aquatic-Product Processing and Preservation, College of Food Science and Technology, Shanghai Ocean University, Shanghai 201306, China

Contact Information:
First author, 857447981@qq.com,
*Corresponding author, jzhong@shou.edu.cn

INTRODUCTION

It's generally accepted that electrospinning, as a simple and promising technique, has been used to fabricate micro- and nanofibers from a variety of polymers. Both coaxial and emulsion electrospinning can be used to make core-shell structural fibers. Compared with coaxial electrospinning, emulsion electrospinning can be easily completed with only one nozzle, without the need for precise control of process variables. Therefore, emulsion electrospinning can provide a simpler method to reduce the burst release of bioactive compounds in the fiber.

AIM

Electrospinning of gelatin/vitamin C stabilized fish oil emulsion was used to prepare core-shell nanofibers, and physical characterization and chemical property determination of fiber membranes were performed.

METHOD

The nanofibers shapes were photographed by a digital camera, an upright optical microscope, a fluorescence microscope, and a scanning electron microscope.

- **For OM observation**, the electrospun fibers were directly collected on microscope glass slides.
- **For FM observation**, Nile Red was added to the gelatin/ Vitamin C/oil mixtures after homogenization and the Nile Red-loaded fish oil emulsion was used to prepare core−shell nanofibers.
- **The peroxide value of fish oil** was determined by the method of ferrus oxidation xylenol orange assay.

RESULTS

Compared with 35% G (0h and 2h), emulsions with different concentrations of VC did not change much (Figure 1 and 2).The results showed that the dyed fish oil is observed to be encapsulated in the fibers in the fluorescence microscope image, proving the core-shell nanofiber structure (Figure 3). Increasing the Vitamin C concentration from 5% to 40% Vitamin C resulted in a smoother surface of the electrospun fiber. It was observed in scanning electron microscope (SEM) images that: 1 day later, compared with the electrospun fiber film formed by emulsion without Vitamin C, except for the adhesion of the fiber film with 40% Vitamin C concentration, the morphology of the fiber film with different Vitamin C concentration basically did not change (Figure 5). The fish oil encapsulated in the emulsion-based fiber mat has an increased antioxidant capacity as the Vitamin C concentration increases (Table 1).

Figure.1. Digital camera of emulsion made with 35% G and different concentrations of vitamin C

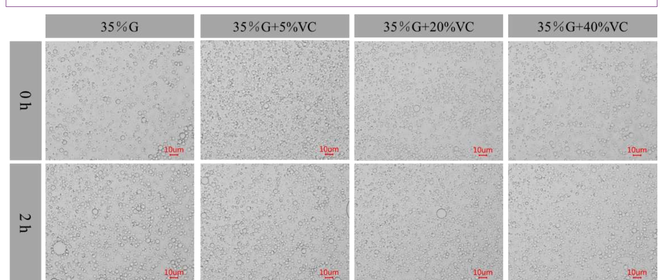

Figure .2. Optical microscope image of emulsion made with 35% G and adding different concentrations of VC

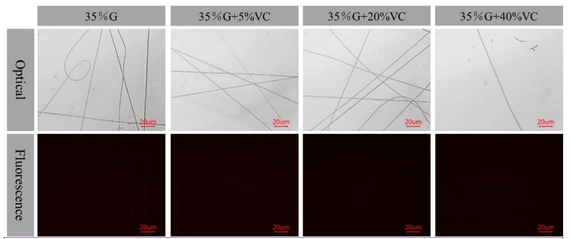

Figure .3. Optical and fluorescence microscopy of electrospun fibers with 35% G and different concentrations of vitamin C emulsion.

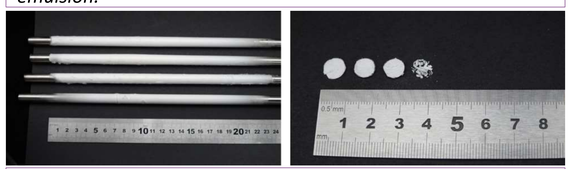

Figure. 4. Digital camera picture of electrospun film (from top to bottom and from left to right: 35%G, 35%G+5%VC, 35%G+20%VC, 35%G+40%VC)

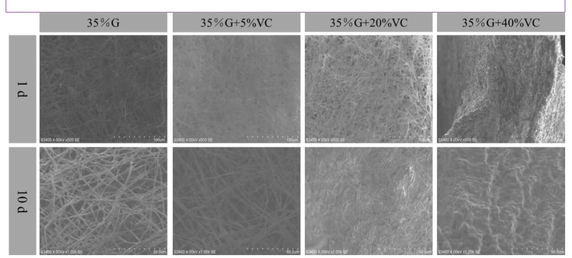

Figure .5. SEM images of emulsion electrospun membranes made of 35% G and adding different concentrations of VC at room temperature for different times (1d and 10d)

Table 1 The absorbance value of 35% G and adding different concentrations of VC electrospun membrane (λ =560nm)

样品(360μL/mL)	35%G	35%G+5%VC	35%G+20%VC
吸光度	1.212	0.567	0.161

CONCLUSIONS

In this work, core-shell nanofibers were prepared by electrospinning a fish oil emulsion stabilized by gelatin/VC. For gelatin-stabilized O/W emulsions, gelatin can quickly diffuse to the newly formed water-oil interface and form a space protein-based barrier. Under a high-voltage electric field, the O/W emulsion can be electrospun to form core-shell nanofibers. The oxidation resistance of electrospun fibers added with VC is improved. In addition, the nanofiber mat has good storage stability and thermal decomposition stability, so it is expected to encapsulate heat-sensitive or hydrophobic bioactive compounds as a controlled release delivery vehicle.

ACKNOWLEDGEMENTS

This research has been supported by research grants from the National Key R&D Program (2019YFD0902003), and Shanghai Municipal Education Commission—Gaoyuan Discipline of Food Science & Technology Grant Support (Shanghai Ocean University).

REFERENCES

[1] Mendes A C , Stephansen K , Chronakis I S . Electrospinning of food proteins and polysaccharides[J]. Food Hydrocolloids, 2016.
[2] Anu Bhushani J , Anandharamakrishnan C . Electrospinning and electrospraying techniques: Potential food based applications[J]. Trends in Food ence & Technology, 2014, 38(1):21-33.
[3] Lingli, Deng, Xi, et al. Characterization of gelatin/zein nanofibers by hybrid electrospinning[J]. Food Hydrocolloids, 2018.
[4] Zhang H , Jia X , Han F , et al. Dual-delivery of VEGF and PDGF by double-layered electrospun membranes for blood vessel regeneration.[J]. Biomaterials, 2013, 34(9):2202-2212.

FSMILE 2020

November 24-25, 2020

P-4

Natural triterpenoids isolated from Akebia trifoliata Stem Explants exerts hypoglycemic effect via inhibits α-glucosidase and stimulates glucose uptake in insulin-resistance HepG2 cells

B. Guoyong 1, C. Yulin 1, W. Ruijie 1, B. Chunling 2, W. Wenhui *1 3, and J. Elango * 1

1 Shanghai Ocean University, Shanghai, China

2 East Branch of Shanghai Sixth People's Hospital Affiliated to Shanghai University of Medicine & Health Sciences, Shanghai, China

3 National R&D Branch Center for Freshwater Aquatic Products Processing Technology, Shanghai, China

Contact Information:

B. Guoyong bgyshou@gmail.com

W. Wenhui whwu@shou.edu.cn

No.999, Huchenghuan Rd , Nanhui New City, Shanghai, P.R. China Zip Code:201306. ShangHai Ocean University

INTRODUCTION

Diabetes mellitus (DM) is a chronic metabolic and heterogeneous disorder, characterized by hyperglycemia that occurs due to abnormal metabolism of lipids, proteins and carbohydrates in terms of insulin resistance or insulin deficiency. The inhibition of α-glucosidase activity is a prospective approach to prevent postprandial hyperglycemia in the treatment of type 2 diabetes mellitus (T2DM).[1-2] **Akebia trifoliata**, commonly called 'san-ye-mu-tong', which has been widely used in the treatment of water-sodium retention disease, and urinary stones in China for hundreds of years. Therefore, the phytochemicals from A. trifoliata have great potential to development of effective and safe agents for the prevention and treatment of diabetes mellitus.[3]

AIM

The objective of this study was to identifying the potential **bioactive triterpenoids** in the stem explants of Akebia trifoliata, and evaluate it's hypoglycemic effects by inhibiting α-glucosidase and enhancing glucose uptake in insulin-resistance (IR) HepG2 cells

METHOD

- **Triterpenoids preparation**: Three triterpenoids have been extraction, isolation and identified by TLC, CC over silica, ODS, Sephadex LH-20, HPLC, and H/C-NMR methods.
- **α-glucosidase inhibition**: Inhibitory activities of three triterpenoids (A-C) against α-glucosidase, and compared with positive control acarbose.
- **kinetics study:** the inhibition mode of three inhibitors on α-glucosidase were determined by the Lineweaver-Burk and Dixon plots.[4]
- **Molecular docking**: Analyzed and visually binding interaction between α-glucosidase enzyme and ligands using Discovery Studio, Pymol, PROCHECK, etc.
- **Glucose uptake**: We evaluate the glucose uptake through monitoring the glucose fluorescent analogue in insulin induced insulin resistance HepG-2 cells.

RESULTS

As shown in figure. 1, three terpenoids had a significant inhibitory ability on α-glucosidase as compared with positive control acarbose. Hederagenin reversibly inhibited glucosidase in a competitive manner with (IC_{50} = 42.1 ± 5.4; K_i = 21.66 μM), showed significant inhibitory power than acarbose. Whereas, 3-Epiakebonoic acid reversibly inhibited enzymatic activity in a mixed manner mode with (IC_{50} = 19.6 ± 3.2 μM; K_i = 7.70 μM; K_{is} = 31.46 μM). Further, the most potent arjunolic acid in a non-competitive manner with (IC_{50} = 11.2 ± 2.3; K_i = 3.18 μM), which possesses stronger inhibitory activity than that of acarbose (IC_{50} = 106.3 ± 7.2 μM).

As shown in figure. 2, Preliminary results on sequence analysis showed that the best template structure//most suitable template for homology model is isomaltase from S. cerevisiae (PDB: 3A4A) which shares 72% identity and 85% similarity with the target enzyme, α-glucosidase of S. cerevisiae.

As shown in figure. 3, The Ramachandran plot obtained from PROCHECK showed that 90.58 % of residues of the final 3D structure lied in most favored regions.

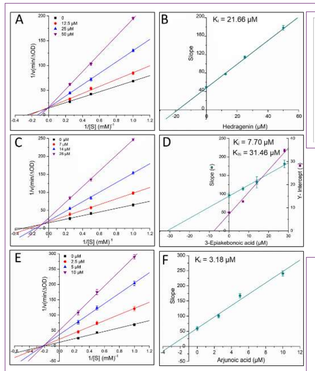

Figure. 1. Lineweaver-Burk plot (A, B, and C) for α-glucosidase inhibition by hederagenin, 3-Epiakebonoic acid, and arjunolic acid, respectively. Results are expressed as mean ± SD (n=6).

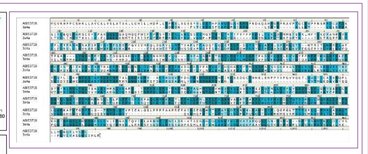

Fig. 2. Sequence alignment of α -glucosidase from S. cerevisiae (UniProt ID: ABI53718.1) and isomaltase from S. cerevisiae (PDB ID: 3A4A).

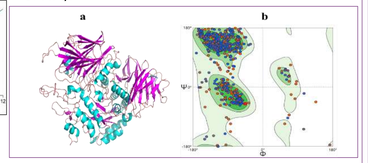

Fig. 3. Homology modelled 3D structure of the selected α-glucosidase (a), and Ramachandran plot (b)

As shown in figure. 4, In silico docking analysis determined the interaction of compounds and α-glucosidase were mainly forced by hydrogen and hydrophobic bonds, which bound to the active site with several key residues, such as Arg154, Ile111, Ala242, Phe240, Phe245, Lys114, Phe159, Ser135, Phe241, Asp243, Glu539, and Asp185, which were predicted by performing a protein-ligand docking simulation.

As shown in figure. 5, IR-HepG-2 cells model were conducted in this study was: 10^{-7} M insulin administered to the HepG2 cells during 24 h. We also examined the glucose uptake property of three terpenoids (A-C) with no cytotoxicity concentrations range from (6.25 - 25 μM), the results revealed that AA and 3-EA can significantly promoting of glucose uptake in insulin-resistant HepG2 cells.

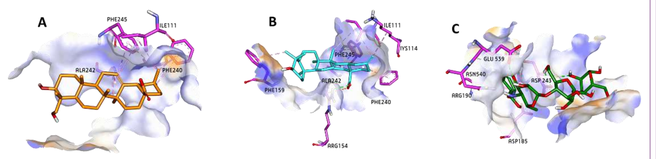

Fig. 4. Ligand interaction diagram of Hederagenin (A), 3-Epiakebonolic acid (B), and Acarbose (C) inside the active pocket of Saccharomyces cerevisiae α-glucosidase.

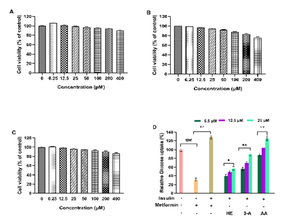

Fig. 5. Effect of compounds on HepG2 cell viability (A-C). Cell viabilities were assessed using an CCK-8 assay. Effect of HE, 3A, and AA on insulin-stimulated glucose uptake in insulin-resistant HepG2 cells (Values were expressed as the mean ±S.D. n = 6 for each group. ### P < 0.001 compared with the control group. * P < 0.05, ** P < 0.01, *** P < 0.001 compared with the model group.

CONCLUSIONS

In conclusion, we extracted three triterpenoids (A-C) phytochemicals from the stem of Akebia, namely hedragenin, 3-Epiakebonoic acid, and arjunolic acid, and we analyzed the inhibitory effect and interaction between compounds and α-glucosidase by enzyme kinetics and molecular docking, and also examined the glucose uptake property in IR-HepG-2 cells. The experiment results showed that three terpenoids phytochemicals had significant inhibitory ability on α-glucosidase compared to the classical inhibitor acarbose. In the results of molecular docking, the ligand compounds were bound to α- glucosidase mainly hydrogen bond and hydrophobic amino acid around the active site was the key to the entry of the ligand compound into the active pocket. In addition, we established the IR-HepG-2 cells model in this study with condition: 10^{-7} M insulin administered to the HepG2 cells during 24 h, and evaluate the glucose uptake through monitoring the glucose fluorescent analogue in IR-HepG-2 model. The results demonstrated that 3-EA and AA could significantly stimulate glucose uptake than positive control metformin. These findings indicate that the stem explants of A. trifoliata rich in bioactive triterpenoids which are promising for exploitation as functional food ingredients or to be developed as effective and safe agents for the prevention and treatment of diabetes mellitus.

ACKNOWLEDGEMENTS

This work received financial support from the National High Technology Research and Development Program of China, the National Natural Science Foundation of, an International Young Scientist Research Fellowship, and the Plan of Innovation Action in Shanghai.

REFERENCES

1. N. H. Cho et al. IDF Diabetes Atlas: Global estimates of diabetes prevalence for 2017 and projections for 2045 Diabetes Res Clin Pract 2018, 138, 271.
2. J. Wada. Et al. Innate immunity in diabetes and diabetic nephropathy. Nat Rev Nephrol 2016, 12, 13.
3. J.K. Ouyang et al. Triterpenoids with α-glucosidase inhibitory activity and cytotoxic activity from the leaves of Akebia. RSC Advances 2018, 8, 40483.
4. M. Y. Ali et al. Didymin, a dietary citrus flavonoid exhibits anti-diabetic complications and promotes glucose uptake through the activation of PI3K/Akt signaling pathway in insulin-resistant HepG2 cells. Chem Biol Interact 2019, 305, 180.

FSMILE 2020

November 24-25, 2020

P-5

Resveratrol and celastrol loaded Collagen dental implants regulate periodontal ligament fibroblast growth and osteoclastogenesis of bone marrow macrophages

W. Ruijie 1, C. Yulin 1, B. Guoyong 1, B. Chunling 2, W. Wenhui *1 3, and J. Elango * 1

1Shanghai Ocean University, Shanghai, China

2East Branch of Shanghai Sixth People's Hospital Affiliated to Shanghai University of Medicine & Health Sciences, Shanghai, China

3National R&D Branch Center for Freshwater Aquatic Products Processing Technology, Shanghai, China

Contact Information:

W. Ruijie 443770598@qq.com

W. Wenhui whwu@shou.edu.cn

Shanghai Ocean University, Shanghai, 201306, China

INTRODUCTION

Gingivitis is the pre-clinical stage of this periodontal disease and leads to damage or inflammation of the supporting and surrounding tissues in teeth. **Collagen** is widely used for dental therapy in several ways such as films, 3D matrix. **Resveratrol (Res)** has excellent osteogenic and osteoinductive properties[1-2] . **Celastrol (Cel)** has been widely used in wound healing due to its excellent biological activities [3].

AIM

The objective of this study is to fabricate collagen film with TCM such as resveratrol and celastrol in order to investigate the human periodontal ligament fibroblasts (HPLF) growth and bone marrow macrophages (BMM) derived osteoclastogenesis. Further, the physicochemical, mechanical and biological activities of collagen-TCMfilms crosslinked by glycerol and EDC-NHS were investigated.

METHOD

- **Collagen film formation**. Six types of collagen composite films were prepared based on two types of crosslinkers and two types of traditional Chinese medicine
- **Films characterization**. The films characterization was observed by Texture analyzer and differential scanning calorimeter and FTIR etc.
- **Microscopic structural analysis of HPLF cells.** Morphological changes of HPLF cells cultured in control and collagen films were observed by SEM.
- **Cell experiment**. The effect of collagen films on HPLF cells was observed MTT assay.
- **Effect of collagen films in osteoclast formation**. The effect of collagen films in osteoclast formation was observed by the BMM was cultured with collagen FFS in presence of osteoclastogenic inducers, RANKL and mCSF.

RESULTS

***As shown in figure 1**, all the collagen films were clear and transparent, however, the films prepared by EN showed slightly opaque than glycerol films.*

***As shown in figure 2**, the tensile strength of collagen film was increased in collagen-EN-Res and collagen-EN-Cel films compared to control, and the addition of Res and Cel reduced the elongation rate of collagen films. The water solubility of collagen films was not significantly affected by either cross linking agents or Chinese medicines, except in CENR film . Biodegradation experiment results showed that in vitro biodegradation rate of collagen film was reduced with the addition of Res and Cel. The anti-oxidant properties of collagen films were improved by Res and Cel both in glycerol and EN crosslinked films compared to the respective control films (P<0.05).*

***As shown in figure 3**, compared to control cells, the collagen crosslinked films had high cell proliferation (P<0.05) (Figure 6). Addition of Res upregulated the HPLF cell proliferation than control cells (P<0.05).*

***As shown in figure 4**, All the films were smooth and compactly packed structures with even surfaces. Cross-sectional areas also showed the smooth distribution of the cross-linking agent, we further investigated the morphological changes of HPLF cells cultured with collagen films (Figure 8) and without collagen films. We found that the cells grown without collagen films were more flatten dense structure, however, the collagen films cultured cells had long spindle-like fibroblast structures.*

***As shown in figure 5** , Compared to the positive control, the collagen films had downregulated osteoclast formation. Besides, the downregulating effect of collagen films was increased with the addition of Res and cel. In both gly and EN crosslinked films, the addition of Cel had high downregulating activity than Res crosslinked films. More specifically, the osteoclast downregulating effect was more pronounced in CENC films than CGC films.*

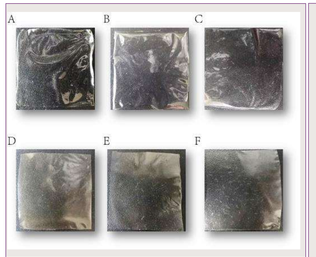

Figure 1.Six type of collagen films prepared with resveratrol and celastrol by glycerol and EN crosslinking. A: CG: collagen-glycerol film, B: CGR: collagen-glycerol-resveratrol film, C:CGC: collagen- glycerol-celastrol film, D:CEN: collagen-EDC-NHS film, E:CENR: collagen-EDC-NHS- resveratrol film, F:CENC: collagen-EDC-NHS-celastrol film.

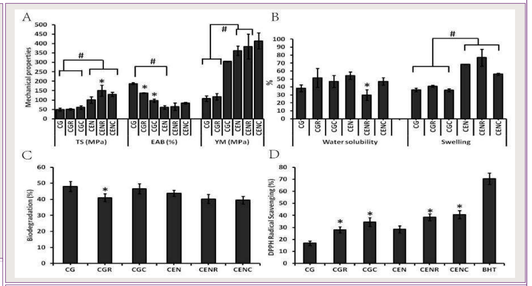

*Figure 2.Mechanical (A), functional (B), biodegradation (C) and antioxidant (D) properties of collagen films.Values are presented as mean +SD, n=3. *P<0.05 vs respective control group. #P<0.05.*

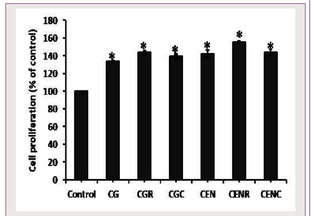

*Figure 3. Effect of collagen composite films in human periodontal ligament fibroblast cells proliferation. The HPLF cells seeded on collagen films for 7 days and cell proliferation was analyzed by MTT assay. Cells were cultured without collagen films as control. Values are presented as mean +SD, n=3,*P<0.05 vs control.*

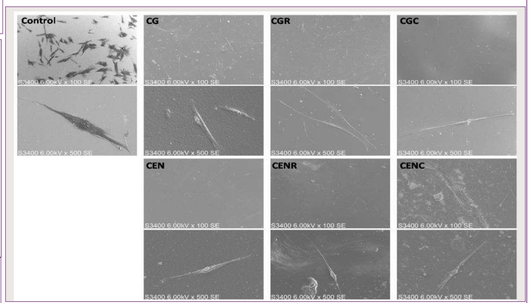

Figure 4. Scanning electron microscopic structure of human periodontal ligament fibroblast cells cultured on collagen composite films.

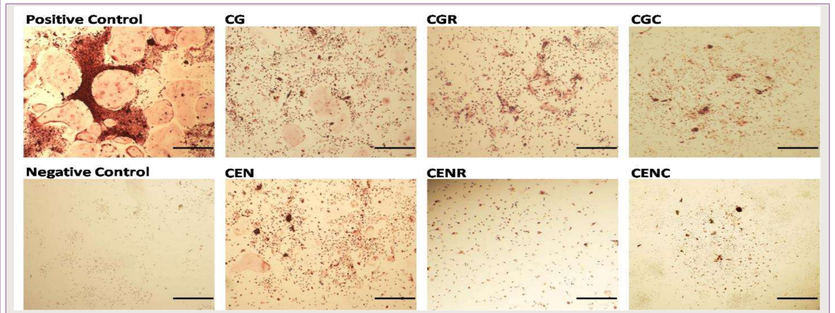

Figure 5.Effect of collagen composite films on mCSF-RANKL induced osteoclastogenesis of bone marrow macrophages. Positive and negative control: BMM cells cultured with and withoutCSF-RANKL, respectively. Scale bars: 200μm.

CONCLUSIONS

The collagen films were prepared by two crosslinking agents and compared their efficiency in traditional Chinese medicine's activity towards dental fibroblast growth. The mechanical properties of collagen films were highly affected by the crosslinking agents especially in terms of stiffness, swelling, denaturation and antioxidant properties of collagen films EN showed a promising effect . SEM images showed the morphological changes of HPLF cells cultured on collagen films and culture plates. The HPLF cell proliferation was upregulated by Res than Cel, the osteoclastogenic formation of BMM was significantly downregulated by Cel compared to Res. Overall the present study concluded that the collagen films combined with traditional Chinese medicine could be the potential biomaterials for dental regeneration after confirming their effect by further in vivo study.

ACKNOWLEDGEMENTS

This work received financial support from the National High Technology Research and Development Program of China, the National Natural Science Foundation of, an International Young Scientist Research Fellowship, and the Plan of Innovation Action in Shanghai.

REFERENCES

1 **K. Bhat et al**. Cancer Chemopreventive Activity of Resveratrol. *Drugs Exp. Clin. Res 1999; 25;: 65-77*

2 **H. Babich et al**. In vitro response of human gingival epithelial S-G cells to resveratrol. *Toxicol. In Vitro 2000; 114;: 143-153.*

3 **J. Zhao et al**. Celastrol-loaded PEG-PCL nanomicelles ameliorate inflammation, lipid accumulation, insulin resistance and gastrointestinal injury in diet-induced obese mice. *J. Controlled Release. 2019; 310;: 188-197.*

4 **J. Elango et al**. Effect of chemical and biological cross-linkers on mechanical and functional properties of shark catfish skin collagen films. *Food Biosci. 2017; 17;: 42-51.*

FSMILE 2020

November 24-25, 2020

P-6

Genomics-based analysis and regulation of the biosynthetic metabolism of FGFC1

C. Yuling 1, B. Guoyong 1, W. Ruijie 1, W. Wenhui *1 2

1 Shanghai Ocean University, Shanghai , Chin

2 National R&D Branch Center for Freshwater Aquatic Products Processing Technology, Shanghai, China

Contact Information:
cao_yuling@163.com

INTRODUCTION

Previous studies genus *Stachybotrys* (*S.*) is a filamentous black mould mainly found in humid environments rich in cellulose. It is feeds by degrading cellulose and other dead plant matter, produces a broad diversity of secondary metabolites, including macrocyclic trichothecenes, atranones, and phenylspirodrimanes.

AIM

De novo sequencing is used to sequence and assemble the genome of a species without relying on a reference genome, so as to draw a complete genome sequence map of the species.

Annotate the gene sequence obtained by sequencing to reveal the biological function and species similarity of *S.longispora FG216*.

METHOD

- **Strains culture and fermentation.** The frozen *S.longispora FG216* are resuscitated, activated and fermented, and the cells are collected, washed twice with PBS, and stored at -20℃.
- **DNA isolation and genome denovo sequencing.** Approximately 1 g of frozen mycelia was grounded to a fine powder with liquid nitrogen, operation was according to the Ezup Column Fungi Genomic DNA Purification Kit instructions.
- **Construction sequencing library.** Next generation sequencing library preparations and Illumina MiSeq sequencing were conducted at GENEWIZ, Inc.
- **Orthologous gene clusters compared.** Analysis of orthologous gene of Stachybotrys including Core gene, Dispensable gene and Specific gene was using the OrthoVenn2.

RESULTS

All the assembled unigenes were subjected to KEGG pathway enrichment analysis. A total of 8422 unigenes (63.19%) could be annotated and assigned to six main categories, which included 379 KEGG pathways (Figure 1b). As can be seen from the figure, the highest number of genes about metabolism matched to the six categories and the lowest number of genes for environmental information processing, yet as a strain of three pathogenic bacteria with distinctly diverse metabolic pathways causing disease in humans.

To obtain a comprehensive insight into cellular function, gene ontology (GO) was performed, resulting in an annotation containing a total of 21,348 unigenes. For biological processes, molecular function and cellular component classes, there are 6335, 12017, 2996 unigenes annotated, respectively. As shown in (Figure 1e), 3319 metabolic processes-related unigenes were detected, along with 1424 unigenes classified within "cellular process" and 1177 unigenes within "localization". Additionally, we found 4156 unigene proteins with a catalytic activity and 3762 unigenes associated with binding function.

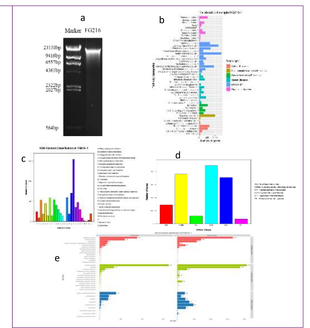

Figure 1.
a. The Genomic DNA extracted from S. longispora FG216 was analyzed by 0.7% agarose.
b. KEGG classifies and statistical the number of genes in each bio metabolic pathways relate to Cellular Processes, Environmental Information Processing, Genetic Information Processing, Human Diseases, Metabolism, and Organismal Systems.
c. Classification of the number of genes annotated by KOG.
d. The CAZy annotation classifies related enzymes as Glycoside Hydrolases (GHs), Glycosyl Transferases (GTs), Polysaccharide Lyases (PLs), Carbohydrate Esterases (CEs), Carbohydrate-Binding Modules (CBM), and Auxiliary Activities (AAs).
e. Gene distribution maps at three GO terms Molecular Function, Biological Process, and Cellular Component reflect the distribution of target genes.

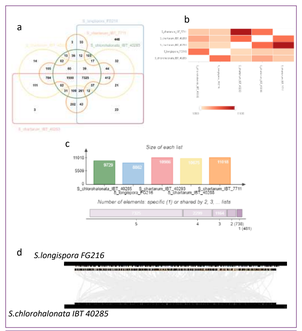

Figure 2.
a. Venn diagram indicating the number of shared orthologous clusters among the genomes of S.longispora FG216, S.chlorohalonata IBT 40285, S.chartarum IBT 40288, S.chartarum IBT 40293 and S.chartarum IBT 7711.
b. Pairwise heatmap of overlapping cluster between pairs of genomes.
c. Summary of protein data of each species.
d. Genome collinearity analysis between S.longispora FG216 and S.chlorohalonata IBT 40285

The predicted genes for the four assemblies (S.chlorohalonata IBT 40285, S.chartarum IBT 40288, S.chartarum IBT 40293, S.chartarum IBT 7711) as well as S.longispora FG216 were assigned into orthologous groups, which resulted in 7325 core gene clusters out of in total 12007 gene clusters, 4866 orthologous clusters (at least contains two species) and 7141 single-copy gene clusters (Figure 2a). S.longispora FG216 showed the 13329 predicted proteomes, but only have 8862 clusters, 3352 proteins are not in any cluster compared to the other four species. S.longispora FG216 has the largest number of 448 specific genes, far more than the other four species.

Figure 2b shows the pairwise heatmap which visualizes the overlapping cluster numbers for five Stachybotrys. S.chartarum IBT 7711 and S.chartarum IBT 40293 shared the highest number of orthologue cluster (10990), followed by S.chartarum IBT 40288 and S.chartarum IBT 40293 (10899) and S.chartarum IBT 40293 and S.chartarum IBT 40288 (10893). However, S.longispora FG216 shared the higher number of orthologue cluster with S.chlorohalonata IBT 40285(10891).

Table 1. *Stachybotrys sp.* genome assembly metrics.

	S.longispora FG216	*S.chartarum*[a]	*S.chartarum IBT 40288*[b]	*S.chartarum IBT 40293*[c]	*S.chartarum IBT 7711*[d]	*S.chlorohalonata IBT 40285*[e]
#scaffolds	605	1,434	2,351	2,342	2,290	2,802
Total length (Mb)	45.6	41.01	36.01	36.48	36.88	34.39
CDS	13,329		11,368	11,453	11,530	10,706
Largest scaffold (Mb)	1.144	4.955	0.433	0.762	0.861	0.484
N50(bp)	295,293	1,219,284	126,356	200,047	176,820	114,117
GC (%)	51.31	51.2	53.4	53.2	53.1	53.2

Table 2. *S.longispora FG216* coding gene prediction statistics.

#Total sequences	Total bases (Mb)	Min length (bp)	Max length(bp)	Average length (bp)	N50(bp)	(G + C)s%	Ns%
13329	21.25	161	32,349	1,594.42	1845	54.72	0

CONCLUSIONS

In this study, the genomic of *S.longispora FG216* was sequenced for the first time using Denovo technology, at the same time the sequencing results were assembled and annotated for coding gene function and preparing for the following molecular biology analysis. Based on the enrichment analysis of the coding genes of KEGG, KOG, GO and CAZy databases, to understand the physiological functions of the strain. The gene function is mainly involved in the metabolic process with catalytic activity, and the secondary metabolites are rich in amino acids, while the metabolism of various functional substances is still to be explored. As a pathogen, it can easily cause various diseases in the human body. Species homology analysis shows that Stachybotrys is a highly conserved species, with a high proportion of shared genes predicting functional similarity, meanwhile *S.longispora FG216* having the highest similarity to *S.chlorohalonata IBT 40285*.

ACKNOWLEDGEMENTS

This work received financial support from the National High Technology Research and Development Program of China, the National Natural Science Foundation of, an International Young Scientist Research Fellowship, and the Plan of Innovation Action in Shanghai.

REFERENCES

[1] Li H. and Durbin R. (2009) Fast and accurate short read alignment with Burrows-Wheeler Transform. Bioinformatics, 25:1754-60. [PMID: 19451168](BWA)

[2] Li H. and Durbin R. (2010) Fast and accurate long-read alignment with Burrows-Wheeler Transform. Bioinformatics, Epub. [PMID:20080505](BWA)

[3] Hyatt D, Chen G L, LoCascio P F, et al. Prodigal: prokaryotic gene recognition and translation initiation site identification[J]. BMC bioinformatics, 2010, 11.(prodigal)

[4] Eric P. Nawrocki, Sarah W. Burge, Alex Bateman, Jennifer Daub, Ruth Y. Eberhardt, Sean R. Eddy, Evan W. Floden, Paul P. Gardner, Thomas A. Jones, John Tate and Robert D. Finn Rfam 12.0: updates to the RNA families database. Nucleic Acids Research (2014) 10.1093/nar/gku1063(Rfam)

[5] Altschul S F, Gish W, Miller W, et al. Basic local alignment search tool[J]. Journal of molecular biology, 1990, 215(3): 403-410.(BLAST)

FSMILE 2020
November 24-25, 2020

Action Mechanism of Chitosan Against *Staphylococcus saprophytic*

Weiqing LAN[1,2,3] Xin YANG[1], Meng WANG[1] Zi-xin FU1 Ze-hui QIU1 Jun MEI[1,2,3] Jing XIE[1,2,3*]

1. College of Food Science and Technology, Shanghai Ocean University, Shanghai 201306, China
2. Shanghai Aquatic Products Processing and Storage Engineering Technology Research Centre, Shanghai 201306, China
3. National Experimental Teaching Demonstration Centre for Food Science and Engineering (Shanghai Ocean University), Shanghai 201306, China

Corresponding author：
Jing XIE. Tel.: 86-21-61900351;
Fax: 86-21-61900365;jxie@shou.edu.cn

INTRODUCTION

- Microorganisms are the main cause of aquatic products spoilage, among which specific spoilage bacteria play a leading role.
- Chitosan is a kind of natural biological preservative, which has a high efficient and broad spectrum killing effect on bacteria.
- *Staphylococcus saprophyticus* is the Specific Spoilage Organism of large yellow croaker, which can cause protein degradation and lipid oxidation, and affect its quality finally.

AIM

The aim is analyze the antibacterial mechanism of chitosan against *Staphylococcus saprophyticus*.

METHOD

Determined minimum inhibitory concentration (MIC) of chitosan .

Chitosan of MIC and 2MIC acted on *Staphylococcus saprophyticus*

Minimum inhibitory concentration (MIC)
Alkaline Phosphatase(AKP)
Microbial growth curve
Electrical conductivit Catalase (CAT)
Malate dehydrogenase (MDH)
Biofilm production
Scanning electron micrographs

RESULTS

Table 1 Effects of chitosan on the growth of *Staphylococcus saprophyticus*

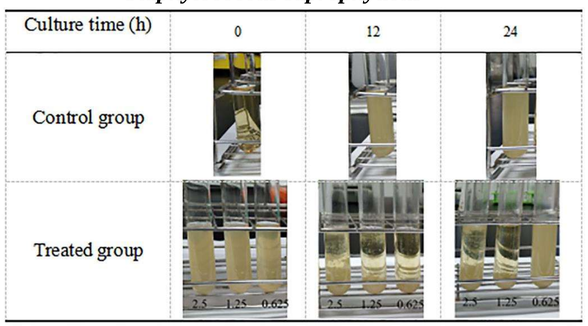

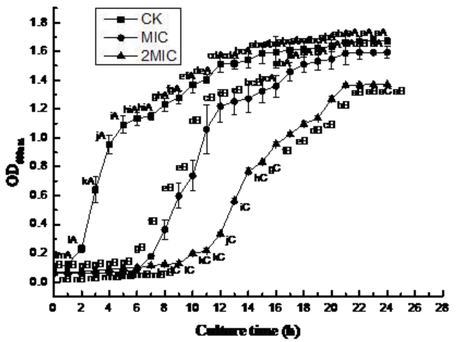

Fig. 1 Effects of chitosan on the growth curve of *Staphylococcus saprophyticus*

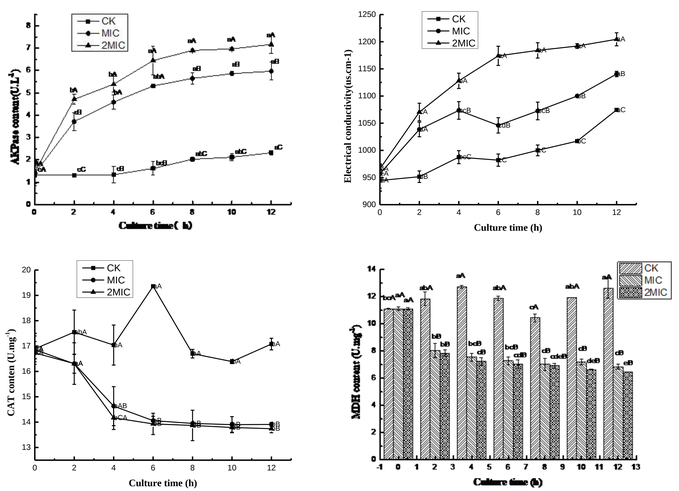

Fig. 2 Effects of chitosan on the AKPase,electrical conductivities,Catalase,Malate dehydrogenase content of *Staphylococcus saprophyticus*

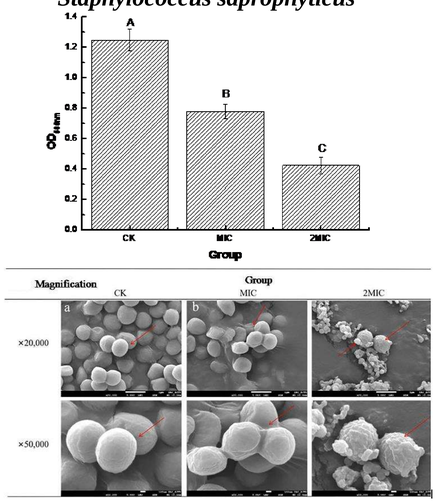

Fig. 3 Effects of chitosan on the biofilm formation of *Staphylococcus saprophyticus* and Scanning electron micrographs

CONCLUSIONS

- The MIC of chitosan against *Saprophylaxis Staphylococcus* was 1.25 mg/mL, and after treatment with MIC and 2MIC, the contents of CAT and MDH decreased, while the conductivity value increased.
- Chitosan can delay the growth of Staphylococcus saprophyticus, inhibit the formation of biofilm.
- Scanning electron micrographs shows chitosan can damage the cell wall structure, enhance the permeability of the cell membrane, and enter the cell, destroy the protective metabolic enzyme system, ultimately lead to the cell death.

ACKNOWLEDGEMENTS

The study was financially supported by National Key R&D Program of China (2019YFD0901602), China Agriculture Research System (CARS-47-G26), Ability promotion project of Shanghai Municipal Science and Technology Commission Engineering Center (19DZ2284000)

REFERENCES

[1] TAOUKIS P S, KOUTSOUMANIS K, NYCHAS G J E. Use of time temperature integrators and predictive modeling for shelf life control of chilled fish under dynamic storage conditions [J]. Int J Food M icrobiol, 1999, 53: 21-31.

[2] BOZIARIS I S, PARLAPANI F F. Chapter 3–Specific Spoilage Organisms (SSOs) in Fish[J]. Microbiological Quality of Food, 2017: 61-98.

[3] ODEYEMI O A, BURKE C M, BOLCH C C J, et al. Seafood spoilage microbiota and associated volatile organic compounds at different storage temperatures and packaging conditions[J]. International Journal of Food Microbiology, 2018, 280: 87-99.

[4] NOSEDA B, ISLAM M T, ERIKSSON M, et al. Microbiological spoilage of vacuum and modified atmosphere packaged Vietnamese Pangasius hypophthalmus fillets[J]. Food Microbiology, 2012, 30(2): 408-419.

[5] ZHANG N, LAN W, WANG Q, et al. Antibacterial mechanism of Ginkgo biloba leaf extract when applied to Shewanella putrefaciens and Saprophytic staphylococcus[J]. Aquaculture and Fisheries, 2018, 3(4): 163-169.

[6] BONILLA F, CHOULJENKO A, LIN A, et al. Chitosan and water-soluble chitosan effects on refrigerated catfish fillet quality[J]. Food Bioscience, 2019, 31: 100426.

[7] ALISHAHI A, ADER M. Applications of Chitosan in the Seafood Industry and Aquaculture: A Review[J]. Food & Bioprocess Technology, 2012, 5(3): 817-830.

[8] DO VALE D A, VIEIRA C B, DE OLIVERIA J M, et al. Determining the wetting capacity of the chitosan coatings from Ucides cordatus and evaluating the shelf-life quality of Scomberomorus brasiliensis fillets[J]. Food Control, 2020, 116: 107329.

[9] VIVEK K P, SIDDH N U, KESHAVAN N, et al. Antimicrobial biodegradable chitosan-based composite Nano-layers for food packaging[J]. International Journal of Biological Macromolecules,2020,157:212-219.

FSMILE 2020

November 24-25, 2020

Effects of dietary protein levels on non-volatile taste substances of swimming crab (*Portunus trituberculatus*)

Ludan Tu1 Xugan Wu2* Xichang Wang1 Wenzheng Shi1*

1Shanghai Ocean University, Shanghai, China

2Shanghai Ocean University, Shanghai, China

上海海洋大學 SHANGHAI OCEAN UNIVERSITY

INTRODUCTION

The main premise of the formulated diet research is to confirm and optimize nutritional parameters. Feed protein level is associated with the breeding effect and the culture cost.

AIM

The aim of this paper is to provide technical support for dietary protein level in fattening feed for swimming crab for the changes in the contents of non-protein nitrogen(NPN), free amino acids(FAAs), nucleotides and inorganic in the female meat of *Portunus trituberculatus* , and the taste substances were evaluated by TAVs and equivalent umami concentration(EUC) methods.

.

METHOD

- Four isoenergetic and iso-fatty experimental diets, recorded as Diet 1~Diet 4 respectively, were formulated containing 32.16%, 36.13%, 39.59%, 41.24% crude protein.
- The contents of FAAs, umami active nucleotides, NPN and inorganic ions were determined and compared by electronic tongue, amino acid autoanalyzer, high performance liquid chromatography(HPLC), nitrogen analyzer and HPLC-Inductively coupled plasma mass spectrometry(HPLC-ICP-MS).

RESULTS

According to the overall information of the sample which compared and distinguished by the electronic tongue, the recognition index was -3, besides, samples overlapped, indicating that the overall taste of swimming crab(average body weight was 10.98±0.28 g) were not significantly influenced by dietary protein level.

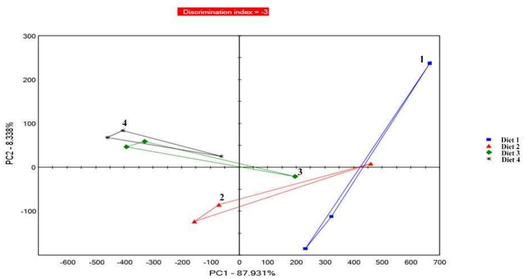

Figure 1 PCA chart for meat of *Portunus trituberculatus* cultured by dietary protein levels

The highest content of NPN, umami and sweet *amino acids, IMP and AMP were observed in the meat of Diet 3. The contents of Ca, K, and Na were not significantly influenced by dietary protein level. And the content of Mg in the diets with 41.24% protein was lower than others. The highest EUC was observed in the Diet 3, suggesting that the umami taste was better.*

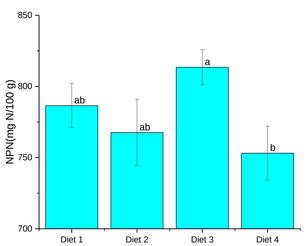

Figure 2 Effects of dietary protein levels on the contents of non-protein nitrogen in meat of *Portuns trituberculatus*

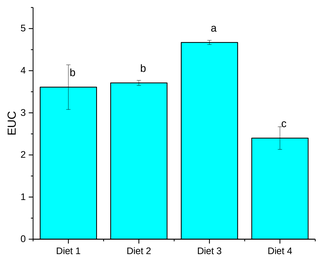

Figure 3 Comparison of EUC in meat of *Portuns trituberculatus* cultured by dietary protein level

Table 1 Effects of dietary protein levels on the contents of inorganic ions in the meat of *Portuns trituberculatus*

Inorganic ions	Content (mg/100 g)			
	Diet 1	Diet 2	Diet 3	Diet 4
Ca	173.50±10.61[a]	157.98±5.66[a]	170.04±7.23[a]	155.44±6.86[a]
K	496.17±4.91[a]	416.75±6.25[a]	435.53±10.56[a]	394.61±13.04[a]
Mg	71.54±3.77[a]	63.13±1.47[ab]	60.29±3.43[ab]	56.34±1.35[b]
Na	509.31±6.37[a]	486.10±10.68[a]	327.52±10.72[c]	428.93±12.15[b]

CONCLUSIONS

Generally, the diet containing 39.59% protein was optimal for swimming crab.

ACKNOWLEDGEMENTS

This study was funded by a Key R&D Program (No. 2018YFD0900100) from Ministry of science and technology of China, an extension project (No. 2016-1-18) from Shanghai Agriculture Committee and a Collaborative Innovation Project for Mari-culture industry in East China Sea from Ningbo University.

REFERENCES

Abdel-Tawwab et al. Effect of dietary protein level, initial body weight, and their interaction on the growth, feed utilization, and physiological alterations of Nile tilapia, Oreochromis niloticus (L.). Aquaculture, 2010, 298;3-4; 267-274

Bibiano Melo, J. F et al. Effects of dietary levels of protein on nitrogenous metabolism of *Rhamdia quelen* (Teleostei : Pimelodidae). Comparative Biochemistry and Physiology a-Molecular & Integrative Physiology, 2006;145;2; 181-187

Catacutan, M. R. Growth and body composition of juvenile mud crab, *Scylla serrata*, fed different dietary protein and lipid levels and protein to energy ratios. Aquaculture, 2002;208;1-2; 113-123

Dai, X et al. Effects of food composition on nitrogen and phosphorus budgets and pollution intensity in Chinese mitten crab (*Eriocheir sinesis*) culture pond. Journal of Hydroecology, 2010;3;; 52-56

He, X et al. Effects of dietary protein levels on growth, ovarian development and biochemical composition of swimming crab(*Portunus trituberculatus*). PROGRESS IN FISHERY SCIENCES, 2020;1-10

FSMILE 2020

November 24-25, 2020

Effects of pectin-plant essential oil on the quality of large yellow croaker (*Pseudosciaena crocea*) with vacuum packaging during iced storage

Weiqing LAN [1,2] Ai LANG[1] Mengling CHEN[1] Jing XIE[*]

1. College of Food Science and Technology, Shanghai Ocean University, Shanghai 201306, China
2. Shanghai Aquatic Products Processing and Storage Engineering Technology Research Centre, Shanghai 201306, China
3. National Experimental Teaching Demonstration Centre for Food Science and Engineering (Shanghai Ocean University), Shanghai 201306, China

Corresponding author：
Jing XIE. Tel.: 86-21-61900351;
Fax: 86-21-61900365
E-Mail: jxie@shou.edu.cn

INTRODUCTION

Oregano essential oil and ginger essential oil have strong antimicrobial and antioxidant properties.

Pectin has characteristics of non-toxic, odorless, renewable, biodegradable, higher solubility in water, good gelation and emulsification stability. In addition, its mechanical resistance, cohesion and stiffness can delay the release of antibacterial agent.

Vacuum packaging is a great way used for the fish preservation due to reduce the deleterious effect of oxygen, and inhibit bacterial growth.

The combination of essential oils, pectin coating and vacuum packaging may preserve fish effectively.

AIM

The aim is extending the shelf life of *Pseudosciaena crocea* with vacuum packaging by using Pectin-Oregano essential oil (PO) and Pectin-Ginger essential oil (PG) coating.

METHOD

Samples:
Fresh large yellow croakers with an average length of 30 ± 2 cm and weight 500± 40 g.
Pectin, oregano essential oil and ginger essential oil were purchased from market.
Experimental design:

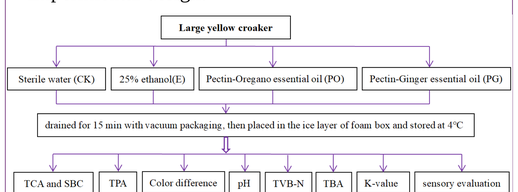

All indexes were analyzed at day 0, 3, 6, 9, 13, 17, 20, 24, 27 respectively.

RESULTS

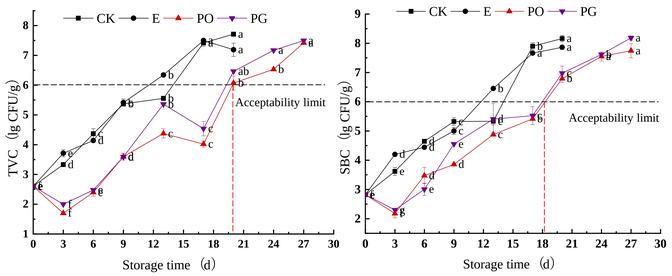

Fig.1 Effects of different treatments on the change of TVC and SBC *Pseudosciaena crocea* with vacuum packaging during ice storage

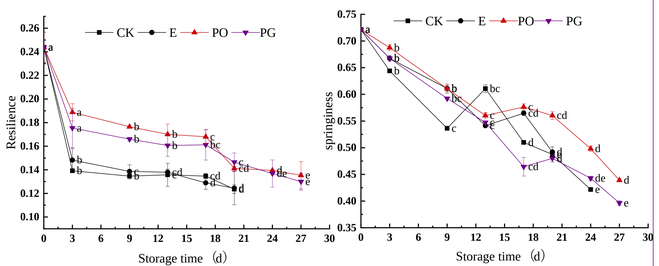

Fig.4 Effects of different treatments on the changes of resilience and springiness in *Pseudosciaena crocea* with vacuum packaging during ice storage

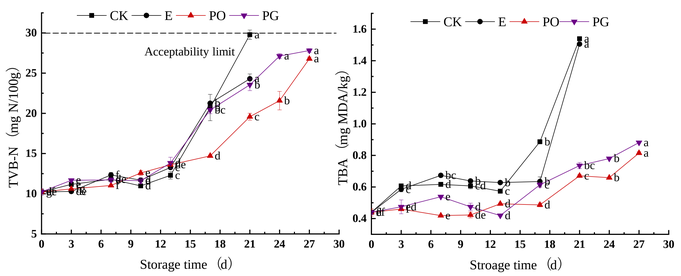

Fig.2 Effects of different treatments on the change of TVB-N and TBA value in *Pseudosciaena crocea* with vacuum packaging during ice storage

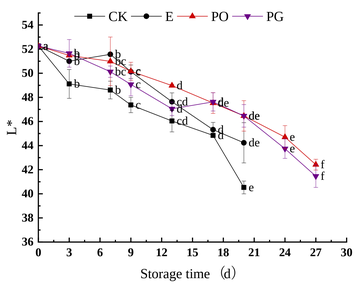

Fig.5 Effects of different treatments on the change of color difference in *Pseudosciaena crocea* with vacuum packaging during ice storage

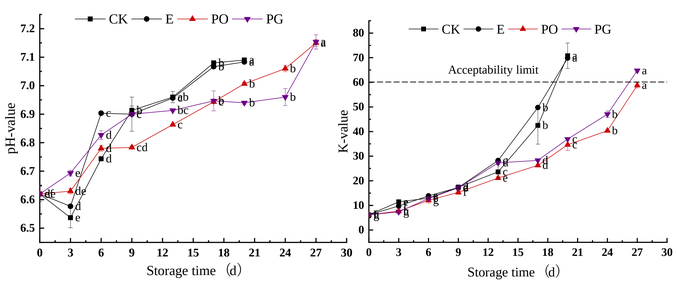

Fig.3 Effects of different treatments on the change of K value and pH value in *Pseudosciaena crocea* with vacuum packaging during ice storage

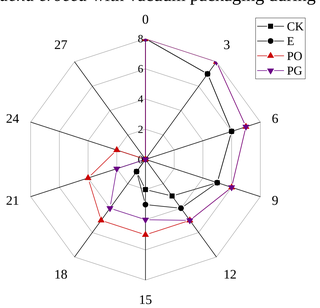

Fig.6 Effects of different treatments on the change of sensory score in *Pseudosciaena crocea* with vacuum packaging during ice storage

CONCLUSIONS

The results showed that PO and PG could inhibit the growth of microorganisms, slow down the lipid oxidation rate, maintain the texture and moisture of the fish, delay the growth rate of TVB-N and K during ice storage, and hinder the spoilage of *Pseudosciaena crocea*.

The preservation effect of PO treatment was better than that of PG group.

PO group and PG can prolong the shelf life of vacuum packaged *Pseudosciaena crocea* from 20 d to 27 d and 24 d respectively, which can be an efficient approach during storage of fishery products to delay the rate of spoilage and will extend the storage life of *Pseudosciaena crocea*.

ACKNOWLEDGEMENTS

The study was financially supported by National Key R&D Program of China (2019YFD0901602), China Agriculture Research System (CARS-47-G26), Ability promotion project of Shanghai Municipal Science and Technology Commission Engineering Center (19DZ2284000)

REFERENCES

1 Thanhhoa, Truonghuynh , L. Baoguo , et al. "Aquaculture Development and Nutrition Management of Large Yellow Croaker (*Pseudosciaena crocea*) in China: An Overview." *Vietnam Journal of Agricultural sciences* 2.4(2020):475-489.

2 A, Haiying Cui, et al. "Antibacterial mechanism of oregano essential oil." Industrial Crops and Products 139. https://doi.org/10.1016/j.indcrop.2019.111498

3 S. Noori, F. Zeynali, H. Almasi, Antimicrobial and antioxidant efficiency of nanoemulsion-based edible coating containing ginger (*Zingiber officinale*) essential oil and its effect on safety and quality attributes of chicken breast fillets. *Food Control* 84 (2018) 312–320.

FSMILE 2020

November 24-25, 2020

P-10

Rapid detection of FWA VBL in flour by in-situ formation of deep eutectic solvent

Qiannan Pan[1], Changhua Xu[1,2,3,*]

1, College of Food Science and Technology, Shanghai Ocean University, Shanghai 201306, China

2, Shanghai Engineering Research Center of Aquatic-Product Processing & Preservation, Shanghai 201306, PR China

3, Laboratory of Quality and Safety Risk Assessment for Aquatic Products on Storage and Preservation , Shanghai 201306, PR China

Contact Information:
chxu@shou.edu.cn

INTRODUCTION

The viscosity, elasticity, whiteness of wheat flour are the standards for evaluating quality of the wheat flour. And the adulterants are subsequently added into the flour illegally and endanger people and needed to be detected effectively.

AIM

Detect the trace FWA VBL in wheat flour effectively by formatting deep eutectic solvent in-situ. Then use the infrared spectroscopy to characterize the formation of DES, use a fluorescence spectrophotometer to quantitatively detect FWA VBL, and apply a scanning electron microscope to obtain the microstructure changes of formation of the DES.

METHOD

1. Sieved wheat flour with 150 meshes
2. Added different contents of FWA VBL into flour
3. Extracted FWA VBL in flour by sonicating and centrifuging
4. Transferred a hydrogen bond acceptor (supernatant) to a hydrogen bond donor (Isobutyl-4-hydroxybenzoate, I4)
5. Mixed under 80℃ and formatted DES in-situ
6. Detected samples by fluorescence spectrophotometry and characterized them by Scanning Electron Microscope (SEM) and Fourier Transform Infrared Spectroscopy (FTIR)

RESULTS

1. FWA VBL in wheat flour could be extracted by formatting deep eutectic solvent (DES) in aqueous solution, which was formatted with I4 (**Fig. 1**).
2. The pre-extracted aqueous solution and the post-extracted aqueous solution were detected by fluorescence spectrophotometry, and the fluorescence intensity of the pre-extracted sample was stronger than it of post-extracted sample (**Fig. 2a**).
3. From the spectra, DES was formed between I4 and FWA VBL through hydrogen. And there were many characteristic peaks of DES showed on the spectra (**Fig. 2b**).
4. From the graphs of SEM, DES was formed a network structure which had regular arrangement between I4 and FWA VBL (**Fig. 3a, Fig. 3b, Fig. 3c, Fig. 3d**).

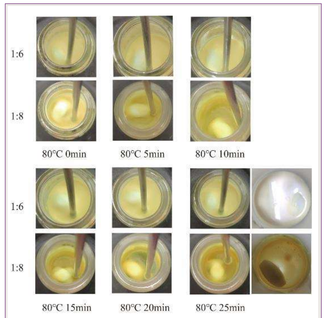

Fig. 1

Fig. 1 *Figure of formation of DES at 80℃ in 25 min with different molar ratio (FWA VBL : I4) 1:6 and 1:8 respectively. The DES could format at ratio 1:8.*

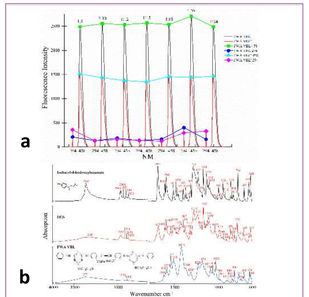

Fig. 2

Fig. 2 *Figures of results of the fluorescence spectrophotometry and the FTIR.* ***a)*** *Graph of pre-extracted and post-extracted of fluorescence spectrophotometry of different molar ratio of FWA VBL and I4.* ***b)*** *Graph of FTIR of I4, DES and FWA VBL and the structures pictures of I4 and FWA VBL.*

Fig. 3 *Graphs of FWA VBL, I4 and DES of SEM.* ***a)*** *The structure of FWA VBL, it showed as snowflake.* ***b)*** *The structure of I4, it showed as rod-shaped.* ***c) & d)*** *The structures of DES, they showed as a network structure with a regular arrangement. The four graphs demonstrated that the FWA VBL and the I4 were combined through hydrogen in the aqueous solution into DES in-situ.*

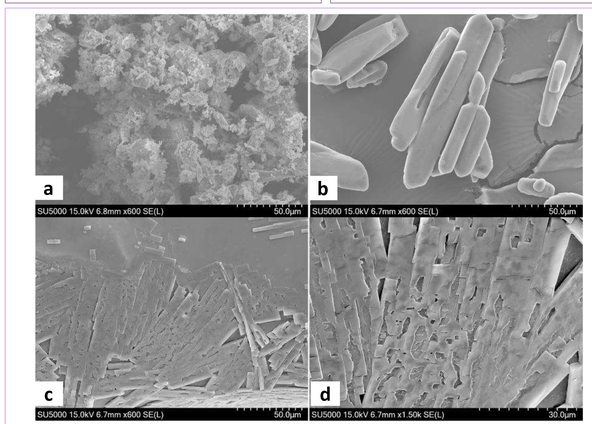

Fig. 3

CONCLUSIONS

From this study, we could conclude that FWA VBL in wheat flour could be extracted by formatting DES in aqueous solution, which was formatted with I4 through the hydrogen. It provided a new method to detect FWA VBL in wheat flour directly and rapidly. Moreover, it also gave a quick way to detect FWAs from the wheat flour and other food through formatting DES in-situ.

ACKNOWLEDGEMENTS

Shanghai Pujiang Program (Grant NO.: 18PJ1432600)

Thermo Fisher Scientific Inc. (Grant No. D-8006-16-0075)

REFERENCES

1.**Shi, Y., et al.** *(2020). "Effective extraction of fluorescent brightener 52 from foods by in situ formation of hydrophobic deep eutectic solvent." Food Chemistry 311: 125870.*

2.**Abbott, A. P., et al.** *(2003). "Novel solvent properties of choline chloride/urea mixtures." The Royal Society of Chemistry 70-71.*

3. **Nail A a , Adil E b , et al.** *(2020). "Alcohol-DES based vortex assisted homogenous liquid-liquid microextraction approach for the determination of total selenium in food samples by hydride generation AAS: Insights from theoretical and experimental studies." Talanta, 215.*

4. **Li X , Row K H .** *(2016). "Development of deep eutectic solvents applied in extraction and separation. " Journal of Separation ence. 39(18).*

5. **Francisco P P, Namienik J .** *(2014). "Ionic Liquids and Deep Eutectic Mixtures: Sustainable Solvents for Extraction Processes." Chemsuschem, 2014, 7.*

FSMILE 2020
November 24-25, 2020

Effects of chitosan combined with apple polyphenols on the microbial diversity of large yellow croaker (*Pseudosciaena crocea*) during ice storage by High-throughput sequencing

Weiqing LAN[1,2,3], Xinyu ZHAO[1], Meng WANG[1], Zixin FU[1] Zehui QIU[1], Jing XIE[1,2,3*]

1. College of Food Science and Technology, Shanghai Ocean University, Shanghai 201306, China
2. Shanghai Aquatic Products Processing and Storage Engineering Technology Research Centre, Shanghai 201306, China
3. National Experimental Teaching Demonstration Centre for Food Science and Engineering (Shanghai Ocean University), Shanghai 201306, China

Contact Information:
Jing XIE. Tel:86-21-61900351;
Fax:86-21-61900365;
Email:jxie@shou.edu.cn.

INTRODUCTION

- Large yellow croaker (*Pseudosciaena crocea*) is an important economic species that favored by consumers.
- Chitosan (CS) is the deacetylated form of chitin and, is a co-polymer of D-glucosamine and N-acetyl-D-glucosaminethe. Apple Polyphenols (AP) is the general term for polyphenols in apples.
- High-throughput sequencing (HTS) can detect both uncultivable microorganisms and low abundance microorganisms

AIM

The aim of this study is investigate to the effects of chitosan (CS) combined with apple polyphenols (AP) on quality and microbial diversity of large yellow croaker (*Pseudosciaena crocea*) during ice storage.

METHODS

Four groups:
(1) Control, sterile distilled water;
(2) AA, 1% Acetic Acid;
(3) CS1+AP, coated with 10.0g/L CS combined with 1.0g/L AP;
(4) **CS2+AP**,coated with 20.0g/L CS combined with 1.0g/L AP

Microbiological, Biogenic amines, HTS analysis

RESULTS

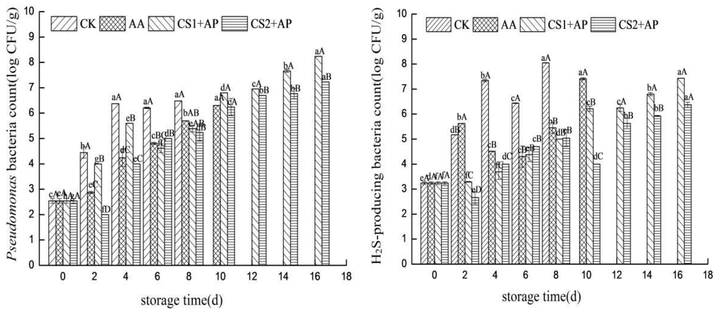

Fig.1. *Pseudomonas* bacteria count (a), H_2S-producing bacteria count (b) of iced large yellow croaker

Tab.1. Changes in biogenic amines (BAs) concentration of iced large yellow croaker .

BAs	Groups	Storage time(day) 0	2	4	6	8	10	12	14	16
Putrescine (mg/kg)	CK	0.58 ± 0.08^{dA}	1.06 ± 0.23^{dA}	6.55 ± 0.06^{cA}	16.07 ± 0.27^{bA}	35.79 ± 0.26^{aA}				
	AA	0.58 ± 0.08^{fA}	0.33 ± 0.27^{fC}	3.09 ± 0.12^{eB}	5.97 ± 0.17^{dB}	10.04 ± 0.19^{cB}	25.45 ± 0.18^{bA}			
	CS1+AP	0.58 ± 0.08^{aA}	0.93 ± 0.12^{fgAB}	1.91 ± 0.33^{fC}	4.29 ± 0.18^{eC}	7.92 ± 0.28^{dB}	8.73 ± 0.28^{dB}	10.79 ± 0.26^{cB}	29.91 ± 0.21^{bA}	33.23 ± 0.32^{aA}
	CS2+AP	0.58 ± 0.08^{fA}	0.82 ± 0.12^{fB}	1.74 ± 0.76^{efC}	2.72 ± 0.22^{eD}	3.14 ± 0.16^{deC}	5.41 ± 0.08^{dC}	7.26 ± 0.06^{cC}	10.09 ± 0.26^{bB}	19.72 ± 0.03^{aB}
Cadaverine (mg/kg)	CK	0.42 ± 0.05^{eA}	0.78 ± 0.12^{dA}	2.14 ± 0.11^{cA}	7.37 ± 0.27^{bA}	15.70 ± 0.25^{aA}				
	AA	0.42 ± 0.05^{fA}	0.51 ± 0.27^{fB}	0.99 ± 0.21^{eB}	2.39 ± 0.18^{dB}	4.82 ± 0.42^{cB}	7.48 ± 0.09^{bA}			
	CS1+AP	0.42 ± 0.05^{bA}	0.36 ± 0.24^{bC}	0.70 ± 0.26^{bC}	1.69 ± 0.18^{fC}	3.88 ± 0.45^{eC}	5.34 ± 0.36^{dB}	8.89 ± 0.17^{cB}	13.05 ± 0.26^{bA}	13.75 ± 0.33^{aA}
	CS2+AP	0.42 ± 0.05^{fA}	0.22 ± 0.28^{fC}	0.31 ± 0.18^{fD}	1.05 ± 0.21^{eD}	3.65 ± 0.11^{dC}	5.09 ± 0.44^{cC}	5.05 ± 0.26^{cC}	9.89 ± 0.33^{bB}	11.97 ± 0.34^{aB}

Tab.2. Species richness and diversity estimators for the gene sequencing within bacterial communities of iced large yellow croaker

Storage time(day)	Groups	Number of Sequence	Number of OTUs	Chao1 index	ACE index	Shannon index	Simpson index	Sequencing depth index
0	CK	21973	150	157.33	155.83	2.92	0.09	0.999
4	CK	85952	209	264.86	274.12	1.19	0.58	0.999
	AA	28098	217	241	225.64	3.29	0.08	0.999
	CS1+AP	17227	366	373.02	378.35	3.85	0.04	0.998
	CS2+AP	9092	258	270.4	275.39	3.36	0.07	0.996
8	CK	40690	177	265.75	360.55	1.74	0.35	0.998
	AA	32237	368	451.02	483.49	1.71	0.38	0.996
	CS1+AP	69754	688	703.59	732.27	1.92	0.31	0.999
	CS2+AP	22481	278	329.09	346.38	1.35	0.56	0.996
10	AA	17283	531	581.53	596.4	2.98	0.27	0.994
16	CS1+AP	55512	154	213.43	311.08	0.34	0.91	0.999
	CS2+AP	44249	238	366.53	494.64	0.27	0.94	0.997

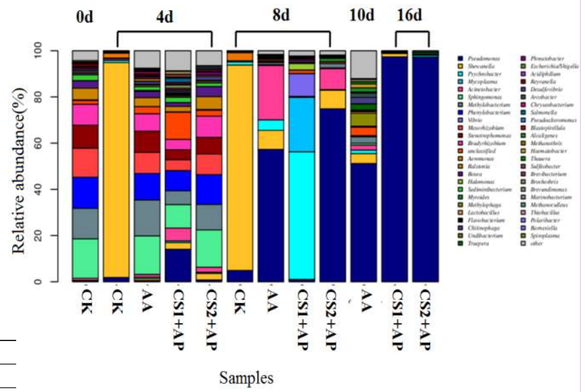

Fig.2. Composition and relative abundance of microbiota at the genus level of iced large yellow croaker

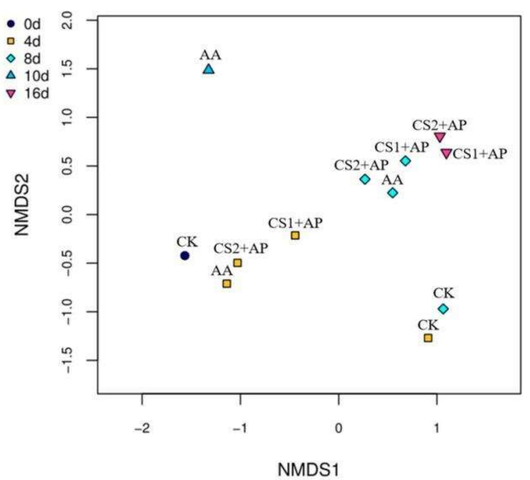

Fig.3. Bacterial community structure of nonmetric multidimensional analysis(NMDS) of iced large yellow croaker

CONCLUSIONS

- CS+AP delayed the quality deterioration of large yellow croaker during ice storage and extended shelf life.
- CS+AP reduced the production of PUT and CAD, and the effect is positively correlated with the concentration of chitosan.
- CS+AP changed the proportion of the dominant bacterium in large yellow croaker.
- CS+AP have the potential to become an effective method for aquatic products preservation.

ACKNOWLEDGEMENTS

The study was financially supported by National Key R&D Program of China(2019YFD0901602), China ;Agriculture Research System (CARS-47-G26); Ability promotion project of Shanghai Municipal Science and Technology Commission Engineering Center.(19DZ2284000)

REFERENCES

[1]**Wang X, Celander M, Yin X, et al**. PAHs and PCBs residues and consumption risk assessment in farmed yellow croaker (*Larimichthys crocea*) from the East China Sea, China.Marine Pollution Bulletin,2019,140:294-300.

[2]**Sun X, Hong H, Jia S, et al.**Effects of phytic acid and lysozyme on microbial composition and quality of grass carp (*Ctenopharyngodon idellus*) fillets stored at 4 °C.Food Microbiology,2020,86:1-10.

[3]**Liu X, Zhang C, Liu S,Gao, et al**. Coating white shrimp (*litopenaeus vannamei*) with edible fully deacetylated chitosan incorporated with clove essential oil and kojic acid improves preservation during cold storage.International Journal of Biological Macromolecules,2020,162:1276-1282.

[4] **Prabhakar P K, Vatsa S, Srivastav P P,et al.** A Comprehensive Review on Freshness of Fish and Assessment: Analytical Methods and Recent Innovations.Food Research International,2020,133:1-17.

FSMILE 2020
November 24-25, 2020

Effects of ice-glazing with rosemary (*Rosmarinus officinalis*) extract on pompano (*Trachinotus ovatus*) preservation during frozen storage

Weiqing LAN[1,2] Lin LIU[1] Taoshuo GONG[1] Xiaohong Sun[1,4] Jing XIE[1,2,3*]
1College of Food Science and Technology, Shanghai Ocean University, Shanghai 201306, China
2Shanghai Aquatic Products Processing and Storage Engineering Technology Research Center, Shanghai 201306, China
3National Experimental Teaching Demonstration Center for Food Science and Engineering (Shanghai Ocean University), Shanghai 201306, China
4Laboratory of Quality＆Safety Risk Assessment for Aquatic Products on Storage and Preservation (Shanghai), Ministry of Agriculture, Shanghai 201306, China

Corresponding author：
Jing XIE.
Tel.: 86-21-61900351
Fax: 86-21-61900365
E-Mail: jxie@shou.edu.cn.

INTRODUCTION

- Pompano (*Trachinotus ovatus*) is enthusiastically welcome due to the palatability and nutrition, but the rich nutrients and moisture make pompano prone to spoilage.
- The Rosemary (*Rosmarinus officinalis*) has excessive antioxidant ability. Glazing is a technique for the purpose of diminishing the undesirable changes of samples during storage.

AIM

There is no report on the combination of rosemary extract(RE) and ice-glazing(IG) during frozen storage. Thus, the objective of this study was to estimate the effect on the quality of pompano when they treated by the RE with IG.

METHOD

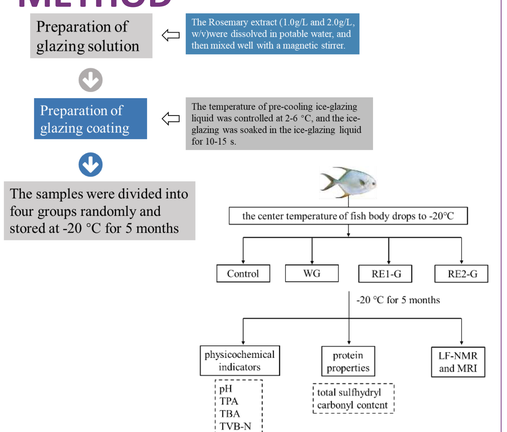

Fig. 1. Experimental flowchart (Control: the unglazed group; WG: sterile water-glazing; RE1-G: 1.0 g/L rosemary extract with ice-glazing; RE2-G: 2.0 g/L rosemary extract with ice-glazing)

RESULTS

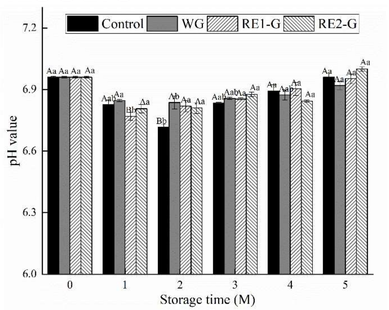

Fig. 2 Effects of different ice-glazing on pH changes of pompano during frozen storage. Different superscript lowercase letters represent significant differences within groups (P<0.05), and different superscript uppercase letters represent significant differences between groups (P<0.05)

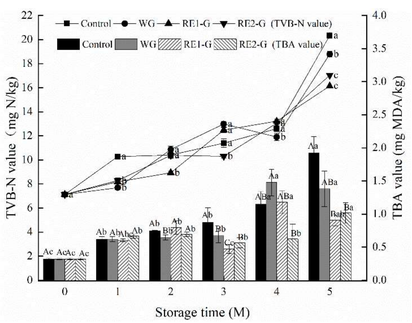

Fig. 3 Effects of different ice-glazing on TVB-N and TBA changes of pompano during frozen storage. Different superscript lowercase letters represent significant differences within groups (P<0.05), and different superscript uppercase letters represent significant differences between groups (P<0.05)

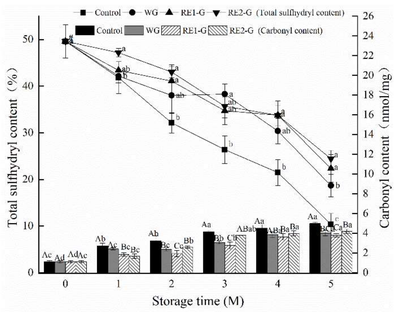

Fig.4 Effects of different ice-glazing on sulfhydryl and carbonyl changes of pompano during frozen storage. Different superscript lowercase letters represent significant differences within groups (P<0.05), and different superscript uppercase letters represent significant differences between groups (P<0.05)

Tab.1 Effects of different ice-glazing methods on TPA changes of pompano during frozen storage

Parameters	Storage time(month)	Group			
		Control	WG	RE1-G	RE2-G
Hardness/g	0	21081.52±102.56^{Ab}	21081.52±102.56^{Ab}	21081.52±102.56^{Ac}	21081.52±102.56^{Ac}
	1	36723.08±102.46^{ABa}	27495.38±179.03^{Ca}	44416.99±137.46^{Aa}	37218.01±110.34^{ABa}
	2	20538.09±173.93^{Cb}	26438.45±192.57^{Ba}	29047.58±189.01^{ABb}	33187.73±117.86^{Aab}
	3	20230.13±179.34^{Bb}	23854.83±168.46^{ABb}	26690.37±185.32^{ABb}	29942.71±123.46^{Ab}
	4	16235.69±198.34^{Cc}	23850.69±170.02^{Bb}	21621.29±191.06^{Bc}	29900.69±186.93^{Ab}
	5	6140.13±167.89^{Bd}	8055.70±186.13^{ABc}	6585.75±189.73^{Bd}	8823.08±97.42^{Ad}
Resilience	0	3305.25±37.45^{Ad}	3305.25±37.45^{Ab}	3305.25±37.45^{Ab}	3305.25±37.45^{Ab}
	1	2286.74±9.45^{Be}	3603.28±46.86^{Aa}	2650.40±45.37^{Bc}	3379.39±15.62^{Ab}
	2	2855.52±38.62^{Be}	2899.44±34.71^{Bc}	2755.94±14.73^{Bc}	3304.60±34.62^{Ab}
	3	5141.48±27.55^{Ac}	2552.98±34.06^{Cc}	4214.42±11.32^{Ba}	4934.67±19.83^{Aa}
	4	6126.84±47.36^{Ab}	3323.98±52.03^{Bb}	2715.78±11.37^{Bc}	2609.49±13.86^{Bc}
	5	7087.64±24.83^{Aa}	3788.49±27.67^{Ba}	3508.35±23.42^{Bb}	2846.24±31.66^{Bc}
Springiness	0	0.53±0.07^{Aab}	0.53±0.07^{Aa}	0.53±0.07^{Aa}	0.53±0.07^{Ab}
	1	0.63±0.11^{Aa}	0.57±0.06^{Aa}	0.59±0.04^{Aa}	0.67±0.05^{Aa}
	2	0.56±0.07^{Aab}	0.54±0.04^{Aa}	0.55±0.03^{Aa}	0.56±0.03^{Aa}
	3	0.42±0.08^{Ab}	0.52±0.04^{Aa}	0.49±0.03^{Ab}	0.52±0.04^{Ab}
	4	0.41±0.08^{Ab}	0.48±0.06^{Ab}	0.48±0.04^{Ab}	0.51±0.03^{Ab}
	5	0.34±0.09^{Bc}	0.37±0.02^{Bb}	0.46±0.05^{Ab}	0.50±0.07^{Ab}

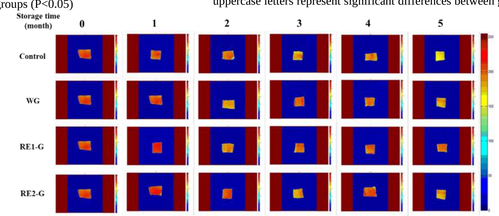

Fig.5 Effects of different glazing on MRI in pompano during frozen storage

Tab.2 Effects of different ice-glazing on the percentage of T2i changes in pompano during frozen storage

Parameters	Group	Storage time (month)					
		0	1	2	3	4	5
pT_{21}	Control	2.80±0.21	6.17±0.09	7.01±0.49	5.54±0.46	5.91±0.90	6.45±0.47
	WG	2.80±0.21	5.35±0.31	6.80±0.11	5.84±0.57	5.90±0.26	5.99±0.31
	RE1-G	2.80±0.21	4.84±0.27	6.16±0.44	5.40±0.07	5.71±0.68	5.47±0.81
	RE2-G	2.80±0.21	4.97±0.35	6.04±0.77	5.19±0.81	5.82±1.01	5.76±0.63
pT_{22}	Control	96.98±0.2	93.44±0.83	92.4±0.80	94.10±0.03	93.78±0.23	92.14±0.23
	WG	96.98±0.2	94.33±0.71	92.62±0.04	93.78±0.40	93.90±0.33	92.88±0.19
	RE1-G	96.98±0.2	95.01±0.33	93.33±0.13	94.36±0.83	93.97±0.28	93.32±0.01
	RE2-G	96.98±0.2	94.81±0.40	93.10±0.28	94.44±0.20	94.04±0.04	93.68±0.13
pT_{23}	Control	0.22±0.04	0.39±0.13	0.59±0.22	0.36±0.06	0.31±0.18	1.41±0.27
	WG	0.22±0.04	0.32±0.06	0.58±0.18	0.38±0.01	0.20±0.14	1.13±0.41
	RE1-G	0.22±0.04	0.15±0.06	0.51±0.14	0.24±0.18	0.32±0.27	1.21±0.50
	RE2-G	0.22±0.04	0.22±0.15	0.86±0.10	0.37±0.11	0.14±0.02	0.56±0.11

CONCLUSIONS

The various indexes in frozen pompano decreased with the extension of storage, but the IG treatment could better delay the degradation of the quality. Besides, the quality of the unglazed samples was significantly reduced at the end of frozen storage, such as protein oxidative denaturation, lipid oxidative damage and water loss. On the contrary, the TVB-N and TBA values of the samples treated by RE combined with IG treatment were lower. Meanwhile, the total SH and carbonyl changes of IG samples were slower, especially the water loss in IG with 1.0 g/L RE (RE1-G) group was smaller. Accordingly, the quality of pompano was more effectively preserved by the RE1-G treatment in this study.

ACKNOWLEDGEMENTS

The study was financially supported by National Key R&D Program of China (2019YFD0901602), China Agriculture Research System (CARS-47-G26), Ability promotion project of Shanghai Municipal Science and Technology Commission Engineering Center (19DZ2284000)

REFERENCES

He Q, Li Z, Yang Z, Zhang Y, et al. A superchilling storage–ice glazing (SS-IG) of Atlantic salmon (*Salmo salar*) sashimi fillets using coating protective layers of Zanthoxylum essential oils (EOs). Aquaculture. 2020;514:734506.

Yan W, Zhang Y, Yang R, et al. Combined effect of slightly acidic electrolyzed water and ascorbic acid to improve quality of whole chilled freshwater prawn (*Macrobrachium rosenbergii*). Food Control. 2020;108.

Shi, J., Lei, Y., Shen, H., et al. Effect of glazing and rosemary (Rosmarinus officinalis) extract on preservation of mud shrimp (*Solenocera melantho*) during frozen storage. Food Chemistry, 2019; 272, 604-612.

Wang X, Geng L, Xie J, Qian Y-F. Relationship Between Water Migration and Quality Changes of Yellowfin Tuna (*Thunnus albacares*) During Storage at 0°C and 4°C by LF-NMR. journal of aquatic food product technology. 2018;27(1):35-47.